## Title

Excitation Functions for Actinides Produced in the Interactions of 31P with 248Cm



## Authors

Leyba, J D
Henderson, R A
Hall, H L
et al.

## Publication Date

1990-04-01

LBL-28929
Preprint

Lawrence Berkeley Laboratory
UNIVERSITY OF CALIFORNIA

Submitted to Physical Review C

# Excitation Functions for Actinides Produced in the Interactions of $^{31}P$ with $^{248}Cm$

J.D. Leyba, R.A. Henderson, H.L. Hall, K.R. Czerwinski,
B.A. Kadkhodayan, S.A. Kreek, E.K. Brady, K.E. Gregorich,
D.M. Lee, M.J. Nurmia, and D.C. Hoffman

April 1990



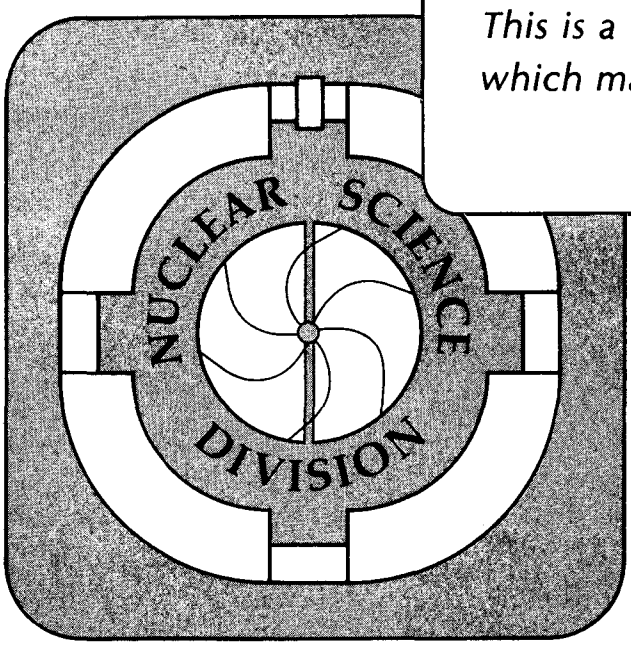




Prepared for the U.S. Department of Energy under Contract Number DE-AC03-76SF00098.

## DISCLAIMER

LBL-28929

# Excitation Functions for Actinides Produced in the Interactions of $^{31}P$ with $^{248}Cm$.

J.D. Leyba, R.A. Henderson, H.L. Hall*, K.R. Czerwinski
B.A. Kadkhodayan, S.A. Kreek, E.K. Brady+, K.E. Gregorich
D.M. Lee, M.J. Nurmia, and D.C. Hoffman

Dept. of Chemistry
University of California
Berkeley, CA 94720

and

Nuclear Science Division
Lawrence Berkeley Laboratory
University of California
Berkeley, CA 94720

April 1990

This work supported in part by the Director, Office of Energy Research, Division of Nuclear Physics of the Office of High Energy and Nuclear Physics of the U.S. Department of Energy under Contract No. DE-AC03-76SF00098.

# Excitation Functions for Actinides Produced in the Interactions of $^{31}P$ with $^{248}Cm$.

J.D. Leyba, R.A. Henderson, H.L. Hall*, K.R. Czerwinski
B.A. Kadkhodayan, S.A. Kreek, E.K. Brady+, K.E. Gregorich
D.M. Lee, M.J. Nurmia, and D.C. Hoffman

Dept. of Chemistry
University of California
Berkeley, CA 94720

and

Nuclear Science Division
Lawrence Berkeley Laboratory
University of California
Berkeley, CA 94720

## ABSTRACT

Excitation functions have been measured for the production of various isotopes of Bk, Cf, Es, and Fm from the interactions of 174- to 239-MeV $^{31}P$ projectiles with $^{248}Cm$. The isotopic distributions were symmetric and displayed full-widths at half-maximum of 2.5, 2.5, <1.5, and 2.25 mass units for Bk, Cf, Es, and Fm respectively. The maxima of the isotopic distributions occur for those reaction channels which involve the exchange of the fewest number of nucleons between the target and projectile for which the calculated excitation energy is a positive quantity. The maxima of the excitation functions occur at those projectile energies which are consistent with the calculated reaction barriers based upon a binary reaction mechanism. The effects of the odd proton in the $^{31}P$ projectile on the final isotopic distributions are discussed.

This work supported in part by the Director, Office of Energy Research, Division of Nuclear Physics of the Office of High Energy and Nuclear Physics of the U.S. Department of Energy under Contract No. DE-AC03-76SF00098.

# I. INTRODUCTION

Transfer reactions continue to be of interest because of their potential usefulness in the production of new neutron-rich actinides. The binary nature of these peripheral reactions makes the production of "cold," neutron-rich actinide nuclei possible. In many instances, the Q values for particular reaction channels are endoergic by 5 MeV or greater. These negative Q values decrease the excitation energy of the targetlike products and afford them a greater probability of surviving fission and/or neutron emission. In addition, the width of the targetlike distributions in A and Z might even make the neutron-rich transactinide region accessible.

Lee et al.[1] initiated a systematic investigation of transfer reactions involving actinide targets and heavy-ion projectiles. The projectile pairs $^{16,18}O$ and $^{20,22}Ne$ were chosen to examine the effects of an extra neutron pair on the final isotopic distributions of the reaction products Bk, Cf, Es, Fm, Md, and No. Lee et al. noted that the two neutron excesses of $^{18}O$ relative to $^{16}O$ and $^{22}Ne$ relative to $^{20}Ne$ were reflected in the final isotopic distributions. As the neutron number of each projectile was increased by two, the corresponding maxima of the mass-yield curves increased by approximately two mass units.

Hoffman et al.[2] sought to extend the study of the influence of neutron excess in the projectile by investigating the effect of the eight neutron excess of $^{48}Ca$ relative to $^{40}Ca$ on the final isotopic distributions from interactions with $^{248}Cm$. The maxima of the isotopic distributions from the $^{48}Ca$ interactions were found to be only 2-3 mass units heavier than the maxima from the $^{40}Ca$ interactions. Hence, only a partial effect of the eight neutron excess of $^{48}Ca$ relative to $^{40}Ca$ was seen in the final isotopic distributions of the above target elements ($Z_{product} > Z_{target}$) Bk, Cf, Es, and Fm.

The $^{44}Ca$-$^{248}Cm$ system was recently studied by Türler et al.[3] $^{44}Ca$ was chosen as a projectile because it has a neutron number (N = 24) which is between the neutron numbers of 20 and 28, respectively of the doubly magic nuclei $^{40}Ca$ and $^{48}Ca$. $^{44}Ca$

was used to investigate the influence of neutron shell effects on the final isotopic distributions. Increases in the mass numbers of the maxima of the isotopic distributions of 0-2 mass units relative to the maxima from the $^{40}Ca$ reactions were found. Consequently, the maxima from the $^{44}Ca$ system fell between the maxima from the corresponding curves in the $^{40}Ca$ and $^{48}Ca$ systems.

Previously we studied[4] the interactions of $^{40}Ar$ with $^{248}Cm$. With this system we observed isotopic distributions which were very similar both in magnitude and in shape to the isotopic distributions from the $^{44}Ca$ system. In addition, the full-widths at half-maximum of the $^{40}Ar$ system were comparable to those from the $^{40}Ca$ and $^{48}Ca$ systems.

Previous transfer reaction studies using $^{248}Cm$ as a target have only used projectiles with even numbers of protons. In order to ascertain any projectile pairing effects on the final isotopic distributions of the heavy actinide transfer products, the odd Z projectile $^{31}P$ (Z = 15) was chosen. Additionally, $^{31}P$ was chosen as a projectile because it has a neutron-to-proton ratio of 1.07, similar to the 1.00 ratio of $^{40}Ca$.

## II. EXPERIMENTAL

The bombardments of the $^{248}Cm$ target were performed at the Lawrence Berkeley Laboratory 88-Inch Cyclotron with 174-, 190-, 207-, 223-, and 239-MeV $^{31}P$ ions. All energies represent the average energy of the $^{31}P$ ions in the target in the laboratory frame of reference and have been corrected for the appropriate energy loss in our target system.[5] The $^{31}P$ ion beam was collimated by water-cooled graphite and passed through a 1.8-$mg/cm^2$ Havar isolation foil which separated the target system from the 88-Inch Cyclotron vacuum system. The beam then passed through 0.2-$mg/cm^2$ $N_2$ cooling gas, a 2.75-$mg/cm^2$ Be target backing foil, and finally the target material.

The target consisted of 0.491-$mg/cm^2$ of $^{248}Cm$ (97.44% $^{248}Cm$, 0.010% $^{247}Cm$, 2.53% $^{246}Cm$, 0.025% $^{245}Cm$, and 1 x $10^{-4}$% $^{244}Cm$) in the form of $Cm_2O_3$. The target was prepared by the stepwise

electrodeposition of Cm from an isopropanol solution onto the Be backing. After approximately 0.07-mg/cm$^2$ had been deposited, the target was baked at 500 °C to convert the Cm to $Cm_2O_3$. The target was then assayed at low geometry with a Si(Au) surface barrier detector to determine its thickness. The electrodeposition, baking, and assaying were continued until the desired thickness was reached.

Gold catcher foils (12.26-mg/cm$^2$) were used to stop and collect the recoiling reaction products. The catcher foils subtended all angles forward of 60° with respect to the beam axis. It was assumed that all of the reaction products recoiled out of the target and were stopped in the catcher foils.

Two irradiations were done at each energy. The first irradiation was a one-hour bombardment from which the Au catcher foil was removed and dissolved in 0.25 ml of hot aqua regia to which a known amount of $^{241}$Am tracer had been added. An ether extraction was performed to remove most of the gold.[6] The resulting aqueous solution was heated in a water bath to remove the dissolved ether and was then passed through a 3-mm-diam by 10-mm-long column of anion exchange resin (Bio Rad AG-1, X-8, 200-400 mesh) to remove the remaining gold. The effluent was evaporated to dryness to remove any residual nitric acid and the remaining activity was dissolved in 3*M* HCl and evaporated on a Pt disc for alpha pulse height analysis. The trivalent actinide chemical yields were determined from the $^{241}$Am tracer.

The second irradiation at each energy lasted between 9.0 and 12.5 hours. The Au catcher foil from each experiment was removed and dissolved in hot aqua regia containing a known amount of $^{241}$Am tracer. An ether extraction was performed, the aqueous solution was heated to remove the dissolved ether, and was then passed through an anion exchange column identical to the one used on the Au foils from the short irradiations. The eluate was evaporated to dryness and fumed twice with concentrated $HClO_4$ to remove any residual organic material. The remaining activity was dissolved in 0.5*M* HCl and sorbed on a 2-mm-diam by 50-mm-long column of cation exchange resin (Dowex-50, X-12, 7-10 μm) maintained at 80 °C. Separate fractions of the trivalent

actinides were eluted with 0.5*M* ammonium alpha-hydroxyisobutyrate (α-HIB) of pH 3.80. The purified chemical fractions were collected on Pt discs in two-drop increments. Those discs containing the same chemical element were combined on a single piece of Pt for pulse height analysis.

A high-purity Ge gamma-ray spectrometer system was used to assay the purified Bk fractions, while the Cf and Fm fractions were assayed with a fission-alpha spectrometer system utilizing Si(Au) surface barrier detectors. For Es, the alpha, spontaneous fission, and gamma activities were assayed simultaneously by mounting the isolated samples in a vacuum chamber which contained a Si(Au) surface barrier detector. The vacuum chamber was then placed next to a Ge(Li) gamma-ray detector. All samples were counted continuously for four weeks after the end of bombardment and then at suitable intervals to provide sufficient data for nuclide identification.

The alpha spectra from each fraction were summed so that even low intensity peaks could be tentatively identified based upon energy. Regions of interest around each peak were set and a simple computer code[7] was then used to integrate the peaks. The SAMPO code[8] was used to analyze the gamma-ray spectra. Decay curve analyses were conducted with the EXFIT[9] and CLSQ[10] computer codes. The activities at the end of bombardment were calculated for each nuclide from the decay curve analyses.

A given nuclide can be produced directly via a transfer reaction or indirectly by the decay of a parent nuclide produced in the bombardment. Hence, in order to obtain the cross section for the transfer reaction, the amount of the nuclide produced via the indirect route(s) must be subtracted from the amount produced directly. After the appropriate corrections were made to the activities at the end of bombardment, the transfer reaction cross sections were calculated. The calculated production cross sections were then corrected for chemical yield and detector efficiencies to obtain absolute cross sections. Because the chemical procedure for the Au catcher foils from the long irradiations required an additional step involving the transfer of elemental fractions from one piece of Pt to another,

the chemical yields of the four purified chemical fractions could not be assumed to be identical to the chemical yield of the $^{241}Am$ tracer. Therefore, the cross sections obtained from the 1-hour irradiations were used to normalize the cross sections from the long irradiations. In addition, cross sections for $^{250}Fm$ ($t_{1/2}$ = 30 m)[11] were obtained from the short irradiations. It is estimated that there is a 12% standard deviation[1] in addition to the statistical standard deviations in the data and decay curve analyses.

## III. RESULTS

The production cross sections along with the statistical standard deviation, *s*, for the measured isotopes of Bk, Cf, Es, and Fm from the interactions of $^{31}P$ with $^{248}Cm$ are listed in Table I and are plotted in Figures 1-4. Because the decay scheme of $^{244}Bk$ has not been measured, its cross sections are based upon the assumption that the abundance of the 217.1 keV gamma ray is 100%; therefore, these values are lower limits only.

### A. Excitation energies

The excess energy available for product excitation, $E_x$ (excitation energy), at the Coulomb barrier for several targetlike and projectile-like fragments from the $^{31}P$ system have been calculated and are listed in Table II. These excitation energies are based upon the entrance and exit channel Coulomb barriers and ground state Q values, assuming two touching spherical nuclei.[12] For reactions with positive excitation energies (of the order of neutron binding energies or fission barriers), the excitation functions should peak near the Coulomb barrier and decrease with increasing projectile kinetic energy. Reactions with negative excitation energies should display excitation functions with maxima at some energy above the Coulomb barrier. The cross sections should then decrease at higher projectile kinetic energy as fission or particle emission becomes energetically possible.

## B. Excitation functions

### *1. Excitation functions for Bk isotopes*

Excitation functions for the Bk isotopes 244,245,246,248*m*, and 250 are shown in Fig. 1. Assuming a binary-type transfer mechanism, the isotope requiring the exchange of the fewest number of nucleons for which $E_X$ is positive (but not large enough to cause fission or neutron emission) should have the highest cross section. $^{249}$Bk meets these requirements. This nuclide requires the transfer of just one proton from the projectile to the target and has an $E_X$ of 6.0 MeV. However, the $^{249}$Bk cross sections were not included for two reasons. First of all $^{249}$Bk is used as a tracer in our laboratory and secondly its measurement is extremely difficult. The difficulty in measurement stems from the fact that the absolute intensities of the most abundant gamma ray and alpha branch from $^{249}$Bk are on the order of 1 X $10^{-5}$. Since $^{249}$Bk has a 99+% $\beta^-$ branch, its activity can be determined from the growth of the $^{249}$Cf daughter. However, the long half-life of $^{249}$Cf ($t_{½}$ = 351 y) makes the detection of this nuclide difficult also. From the experimental data it can be seen that $^{248m}$Bk has the highest cross sections at all energies, with $^{246}$Bk next, followed by $^{250}$Bk, $^{245}$Bk, and finally $^{244}$Bk. All of the Bk excitation functions have maxima at about 207 MeV. The shapes of the excitation functions of $^{244}$Bk and $^{248m}$Bk are consistent with their positive excitation energies. $^{245}$Bk, $^{246}$Bk, and $^{250}$Bk have excitation functions which are very similar in shape. They increase by about a factor of three between 174 and 207 MeV and then show a decrease by more than a factor of two over the next 32 MeV. The shapes of the excitation functions of $^{245}$Bk and $^{246}$Bk, however, do not appear to be consistent with their calculated positive excitation energies. Since their $E_X$'s are positive, one would not expect an increase in the cross sections at the lower bombarding energies.

### 2. *Excitation functions for Cf isotopes*

Excitation functions for the various Cf isotopes measured in this study are shown in Fig. 2. $^{250}$Cf has the highest cross sections, followed by $^{248}$Cf, $^{246}$Cf, $^{252}$Cf, and finally $^{253}$Cf. $^{250}$Cf requires the transfer of the fewest number of nucleons, two protons, and additionally it has an $E_X$ of 7.2 MeV. $^{248}$Cf has much higher cross sections than $^{252}$Cf even though both require the transfer of four nucleons. In fact, $^{252}$Cf can be produced by the transfer of an alpha particle from the projectile to the target. However, $^{248}$Cf has an $E_X$ of 8.8 MeV while $^{252}$Cf has an $E_X$ of only 0.6 MeV. This could explain the lower yields of $^{252}$Cf relative to $^{248}$Cf. The $^{248}$Cf, $^{250}$Cf, and $^{252}$Cf excitation functions have similar shapes, consistent with their positive $E_X$'s. However, for $^{253}$Cf, the cross section at the Coulomb barrier is near its maximum and decreases with increasing projectile energy, inconsistent with its $E_X$ of -8.1 MeV. Finally, $^{246}$Cf has an excitation function which is consistent with a negative $E_X$ value even though this nuclide has an $E_X$ of 6.9 MeV.

### 3. *Excitation functions for Es isotopes*

Fig. 3 shows excitation functions for the Es isotopes 251, 252, 253, 254, and 255. The highest cross sections occur for $^{251}$Es, the isotope requiring the transfer of the fewest number of nucleons (three protons). As the number of nucleons transferred increases, the cross sections decrease. In addition, the shapes of the excitation functions are consistent with their calculated excitation energies.

### 4. *Excitation functions for Fm isotopes*

Excitation functions for various isotopes of Fm are shown in Fig. 4. The shapes of the curves are all similar and again they are consistent with the calculated positive excitation energies. $^{252}$Fm, the Fm isotope requiring the transfer of the fewest number of nucleons (four protons) has the highest cross sections with

$^{256}$Fm, which requires the transfer of eight nucleons, having the lowest cross sections. $^{255}$Fm seems to be an exception in this case. Even though it requires the transfer of seven nucleons, it has higher cross sections at three energies than both $^{254}$Fm and $^{250}$Fm which each require the transfer of six nucleons. The higher cross sections of $^{255}$Fm relative to $^{254}$Fm and $^{250}$Fm cannot be explained on the basis of excitation energies. $^{255}$Fm has an $E_X$ which is 1.9 MeV as compared to 6.2 MeV and 2.4 MeV for $^{254}$Fm and $^{250}$Fm respectively. However, it should be noted that the $^{255}$Fm cross sections have relatively large errors.

### C. Calculation of $F_t$

We have attempted to estimate the fraction, $F_t$, of the projectile kinetic energy transformed into targetlike fragment excitation energy using the equation

$$F_t = (E_{f,n} - E_X)/(E_M - E_B),$$

where $E_{f,n}$ is the height of the fission barrier[13,14] or the neutron binding energy[15] in MeV, whichever is lower, $E_X$ is the excess energy available for product excitation described earlier, $E_M$ is the maximum in the experimental excitation functions, and $E_B$ is the calculated Coulomb barrier assuming two touching spheres. In using this formula, we are assuming that the maximum in the experimental excitation function occurs when the targetlike product excitation energy is comparable to the fission barrier or neutron binding energy. This calculation is not applicable when the reaction energy is greater than the neutron binding energy or the fission barrier, because enough energy is available to cause depletion of the cross section by fission or neutron emission. Table III lists the calculated $F_t$ values for the $^{31}$P system. The $F_t$'s from the $^{31}$P system range in value from 0.01 to 0.69, similar to the values from the $^{40}$Ar and $^{44}$Ca systems.[4] No obvious trends in the $F_t$'s can be seen.

By assuming that the fraction of energy transferred is proportional to the mass transferred, the fraction of energy

transferred, $E_t$, can be calculated according to the equation

$$E_t = M/A,$$

where $M$ is the total number of nucleons transferred and $A$ is the mass number of the projectile. The $E_t$ values are also listed in Table III. There is good agreement between $F_t$ and $E_t$ for $^{252}$Cf, $^{255}$Es, $^{255}$Fm, and $^{256}$Fm. However, there are significant deviations for $^{250}$Bk, $^{253}$Cf, $^{254m}$Es, $^{250}$Fm, and $^{253}$Fm.

## D. Isotopic distributions

### *1. General features*

Isotopic distributions for Bk, Cf, Es, and Fm produced from the interactions of 207-MeV (1.17 X Coulomb barrier) $^{31}$P ions with $^{248}$Cm are plotted in Fig. 5. This energy was chosen so that the $^{31}$P system could be compared to other systems at the same energy relative to the entrance channel Coulomb barrier. All of the data points for each element are connected with lines. These lines are included only to aid the eye in viewing the plot. The isotopic distributions have maxima at $^{248m}$Bk, $^{250}$Cf, $^{251}$Es, and $^{252}$Fm. As stated earlier, all of these nuclides correspond to the isotope requiring the exchange of the fewest number of nucleons for a given element, except in the case of $^{248m}$Bk. All of the curves appear to be symmetric with full-widths at half-maximum (FWHM) of 2.5, 2.5, <1.5, and 2.25 mass units for Bk, Cf, Es, and Fm respectively. Since only upper limits were set on the $^{249}$Es, and $^{250}$Es cross sections, only an upper limit can be set on the FWHM of the Es curve. Additionally, the maxima and the widths of the mass-yield curves stay constant over the energy range investigated.

### *2. Comparison with other systems*

The maxima of the isotopic distributions for the $^{31}$P, $^{40}$Ar, $^{40}$Ca, $^{44}$Ca, and $^{48}$Ca systems are listed in Table IV,[2,3,4]

along with the neutron-to-proton ratios of the projectiles. All of the systems show maximum cross sections for Bk at mass 248 except for the most neutron-deficient projectile, $^{40}$Ca, for which the maximum occurs at mass 247. The maximum cross section for Cf occurs at mass 250 except for the $^{40}$Ca system again, for which its maximum is at 248. The maxima of the Es curves are at mass 251 for $^{31}$P, $^{40}$Ar, and $^{44}$Ca, at 250 for $^{40}$Ca, and at 252 for $^{48}$Ca. The Fm curves have their maxima around 252 in every case except for $^{48}$Ca which has its maxima at 255. It should be noted that the maximum cross sections from the $^{40}$Ar and $^{44}$Ca systems could not be located with certainty due to insufficient data on the neutron-deficient Fm isotopes.

The values of the FWHM's for the $^{31}$P system agree quite well with those reported previously for other systems. Specifically, Lee et al. reported the FWHM's of the $^{16,18}$O and $^{20,22}$Ne systems to all be about 2.5 mass units, while 2.5 and ≈ 2.5 mass units were reported for the $^{48}$Ca and $^{40}$Ca systems respectively.[1,2] Earlier we reported the FWHM's for the $^{40}$Ar and $^{44}$Ca systems to be 2.5-3.25 mass units and 2.0-3.5 mass units respectively.[4]

The final isotopic distributions for Bk from the interactions of various heavy ions (HI) with $^{248}$Cm are shown in Fig. 6. The $^{31}$P system has the highest production cross sections for $^{248m}$Bk by about a factor of 2. This high peak cross section for $^{248m}$Bk might be due to the odd proton in $^{31}$P. Since an odd proton would be unpaired in the nucleus, the probability of transferring 1 unpaired proton from an odd $Z$ nucleus to the target should be greater than the probability of transferring one proton from an even $Z$ nucleus. The calculated $E_X$'s for some Bk isotopes produced from the interactions of $^{18}$O, $^{31}$P, $^{40}$Ar, $^{40}$Ca, $^{44}$Ca, and $^{48}$Ca with $^{248}$Cm are listed in Table V. The $E_X$ values from the $^{31}$P system are greater than the corresponding values from the $^{18}$O, $^{40}$Ar, $^{44}$Ca, and $^{48}$Ca systems. However, the $^{40}$Ca system has $E_X$ values that are greater than those of the $^{31}$P system. This should be expected since the neutron-to-proton ratio of $^{40}$Ca is only 1.00. With such a low neutron-to-proton ratio, $^{40}$Ca should preferentially transfer protons to the target nucleus. The neutron-deficient Bk isotope yields are essentially

independent of the projectile whereas the neutron-rich Bk isotopes are projectile dependent. $^{48}Ca$, the most neutron-rich projectile gives the highest yields and $^{40}Ca$, the most neutron-deficient projectile, gives the lowest yields of the neutron-rich Bk isotopes.

Isotopic distributions for Cf from the reactions of various heavy ions with $^{248}Cm$ are shown in Fig. 7. Again, the yields for the neutron-deficient Cf isotopes are independent of the projectile, except for the yields from the neutron-rich $^{48}Ca$, which has the lowest cross sections. The cross sections for the neutron-rich Cf isotopes are all quite similar for $^{31}P$, $^{40}Ar$, $^{44}Ca$, and $^{48}Ca$. The most neutron-deficient projectile, $^{40}Ca$, is the exception with the lowest cross sections for the neutron-rich Cf isotopes.

Isotopic distributions for Es produced from the interactions of some heavy ions with $^{248}Cm$ are shown in Fig 8. $^{40}Ar$ consistently has the highest yields for the isotopes $^{250-254}Es$. The curve from the $^{31}P$ system seems to have the narrowest FWHM.

Fig. 9 illustrates the final isotopic distributions for Fm produced from the interactions of various heavy ions with $^{248}Cm$. $^{40}Ar$ has the highest cross sections for the neutron-rich Fm isotopes, even though $^{44}Ca$ and $^{48}Ca$ have greater neutron-to-proton ratios. $^{48}Ca$ has the lowest cross sections for the neutron-deficient Fm isotopes.

## IV. Summary

The following conclusions can be made from the present study:

1. In general the cross sections decrease as the number of nucleons transferred increases.

2. Except for $^{245}$Bk, $^{246}$Bk, $^{246}$Cf, and $^{253}$Cf, the shapes of the excitation functions are consistent with the calculated excitation energies.

3. For the $^{31}$P system, the maxima of the isotopic distributions occur for those reaction channels which involve the exchange of the fewest number of nucleons for which $E_x$ is positive. This lends support to a binary-type reaction mechanism in which the targetlike fragment has little excitation energy.

4. The odd proton in $^{31}$P does not have a noticeable effect on the final isotopic distributions of the $^{31}$P system. A possible exception could be $^{248m}$Bk, which has a peak production cross section about a factor of 2 higher than the peak production cross sections for $^{248m}$Bk from other heavy ion-$^{248}$Cm systems.

5. The neutron-rich projectiles such as $^{48}$Ca enhance the production of neutron-rich products while the neutron-deficient projectiles such as $^{40}$Ca and $^{31}$P enhance the production of neutron-deficient products.

## ACKNOWLEDGMENTS

The authors wish to thank the staff and crew of the Lawrence Berkeley Laboratory (LBL) 88-Inch Cyclotron for their assistance. The authors are indebted for the use of the $^{248}Cm$ to the Division of Chemical Sciences, Office of Basic Energy Sciences, U.S. Department of Energy, through the transplutonium element production facilities at the Oak Ridge National Laboratory. This work was supported in part by the Director, Office of Energy Research, Division of Nuclear Physics of the Office of High Energy and Nuclear Physics of the U.S. Department of Energy under Contract No. DE-AC03-76SF00098.

## REFERENCES

*Present address: Nuclear Chemistry Division L-396, Lawrence Livermore National Laboratory, Livermore, CA 94550

+Present address: Department of Chemistry, Beloit College, Beloit, WI 53511

[1]D. Lee, H.R. von Gunten, B. Jacak, M. Nurmia, Y. Liu, C. Luo, G.T. Seaborg, and D.C. Hoffman, Phys. Rev. C 25, 286 (1982).

[2]D.C. Hoffman, M.M. Fowler, W.R. Daniels, H.R. von Gunten, D. Lee, K.J. Moody, K. Gregorich, R. Welch, G.T. Seaborg, W. Brüchle, M. Brügger, H. Gäggeler, M. Schädel, K. Sümmerer, G. Wirth, Th. Blaich, G. Herrmann, N. Hildebrand, J.V. Kratz, M. Lerch, and N. Trautmann, Phys. Rev. C 31, 1763 (1985).

[3]A. Türler, H.R. von Gunten, J.D. Leyba, K.E. Gregorich, R.M. Chasteler, R.A. Henderson, D.A. Bennett, C.M. Gannett, H.L. Hall, R.B. Chadwick, D.M. Lee, M. Nurmia, and D.C. Hoffman, (to be submitted to Phys. Rev. C).

[4]J.D. Leyba, R.A. Henderson, H.L. Hall, C.M. Gannett, R.B. Chadwick, K.R. Czerwinski, B.A. Kadkhodayan, S.A. Kreek, G.R. Haynes, K.E. Gregorich, D.M. Lee, M.J. Nurmia, and D.C. Hoffman, Phys. Rev. C, (to be published).

[5]L.C. Northcliffe and R.F. Schilling, Nucl. Data Tables A 7, 233 (1970).

[6]F. Mylius and C. Hüttner, Bec. Deut. Chem. Ges. 44, 1315 (1911).

[7]H.L. Hall (unpublished).

[8]J.T. Routti and S.G. Prussin, Nucl. Instrum. Methods 72, 125 (1969).

[9]K.E. Gregorich, Ph.D. thesis, University of California, Berkeley, 1985.

[10]J.B. Cumming, Brookhaven National Laboratory Report BNL-6470, 1963.

[11]E. Browne, J.M. Dairiki, R.E. Doebler, A.A. Shihab-Eldin, L.J. Jardine, J.K. Tuli, and A.B. Buyrn, *Table of Isotopes*, edited by C.M. Lederer and V.M. Shirley (John Wiley and Sons, New York, 1978).

[12]D.C. Hoffman and M.M. Hoffman, Los Alamos National Laboratory Report LA-UR-82-824, March 1982.

[13]H.C. Britt, in *Proceeding of the Fourth International Atomic Energy Agency Symposium on Physics and Chemistry of Fission, Jülich, 1979* (IAEA, Vienna, 1980), Vol. I, p. 3.

[14]H.C. Britt, E. Cheifetz, D.C. Hoffman, J.B. Wilhelmy, R.J. Dupzyk, and R.W. Lougheed, Phys. Rev. C 21, 761 1980.

[15]P.A. Seeger, and R.C. Perisho, Los Alamos Scientific Laboratory Report LA-3751, September 1967.

TABLE I. Cross sections from the bombardment of $^{248}Cm$ with $^{31}P$.

| | 174 MeV | | 190 MeV | | 207 MeV | | 223 MeV | | 239 MeV | |
|---|---|---|---|---|---|---|---|---|---|---|
| Nuclide | Cross Section (μb) | *s* (%) | Cross Section (μb) | *s* (%) | Cross Section (μb) | *s* (%) | Cross Section (μb) | *s* (%) | Cross Section (μb) | *s* (%) |
| Bk 244 | 20.3 | 0.7 | 23.7 | 2.2 | 37.9 | 3.1 | 7.20 | 50 | <2.96 | - - - |
| 245 | 224 | 7.1 | 452 | 1.1 | 726 | 1.4 | 436 | 3.4 | 189 | 2.5 |
| 246 | 829 | 1.6 | 1910 | 1.0 | 2590 | 1.2 | 1830 | 2.2 | 1090 | 1.1 |
| 248*m* | 4270 | 1.6 | 7100 | 3.5 | 8680 | 12 | 3880 | 47 | 3590 | 50 |
| 250 | 486 | 1.4 | 991 | 1.0 | 1330 | 1.1 | 1050 | 1.9 | 552 | 1.3 |
| 251 | <6.25 | - - - | <2.57 | - - - | <5.23 | - - - | <34.4 | - - - | <7.88 | - - - |
| Cf 246 | 31.4 | 0.5 | 71.9 | 0.5 | 125 | 0.5 | 75.9 | 0.3 | 44.8 | 0.3 |
| 248 | 892 | 1.1 | 1450 | 1.2 | 2340 | 1.1 | 1640 | 0.8 | 824 | 1.1 |
| 250 | 2850 | 0.6 | 3460 | 0.4 | 5410 | 0.5 | 3790 | 0.5 | 2270 | 0.9 |
| 252 | 50.1 | 8.5 | 73.6 | 4.2 | 105 | 5.9 | 75.9 | 7.8 | 29.4 | 12 |
| 253 | 2.98 | 14 | 3.45 | 15 | 3.15 | 30 | 1.10 | 25 | 0.81 | 14 |
| Es 249 | <6.71 | - - - | <2.75 | - - - | <8.73 | - - - | <18.1 | - - - | <27.8 | - - - |
| 250*m* | <11.6 | - - - | <5.84 | - - - | <43.9 | - - - | <35.4 | - - - | <33.7 | - - - |
| 250*g* | <35.1 | - - - | <48.4 | - - - | <2.34 | - - - | <2.85 | - - - | <4.28 | - - - |
| 251 | 113 | 4.3 | 258 | 2.8 | 179 | 4.1 | 83.9 | 5.8 | 59.4 | 10 |
| 252 | 27.5 | 58 | 89.6 | 7.3 | 68.9 | 9.8 | 37.8 | 13 | 21.5 | 8.8 |
| 253 | 4.22 | 15 | 7.26 | 5.0 | 5.23 | 7.6 | 3.11 | 8.5 | 2.10 | 6.0 |
| 254*m* | 0.074 | 11 | 0.21 | 3.8 | 0.17 | 4.1 | 0.097 | 11 | 0.078 | 7.1 |
| 255 | <0.01 | - - - | 0.006 | 53 | 0.011 | 45 | 0.018 | 54 | 0.005 | 69 |
| Fm 250 | 1.12 | 15 | 1.13 | 8.1 | 1.79 | 15 | 0.17 | 10 | 0.13 | 64 |
| 252 | 7.46 | 58 | 12.1 | 21 | 14.9 | 2.7 | 4.68 | 11 | 1.37 | 22 |
| 253 | 5.99 | 2.2 | 9.71 | 0.8 | 9.97 | 5.0 | 2.65 | 2.7 | 0.69 | 10 |
| 254 | 0.96 | 5.3 | 2.09 | 2.4 | 1.59 | 4.4 | 0.56 | 7.7 | 0.16 | 12 |
| 255 | 1.96 | 58 | 4.11 | 51 | 0.79 | 36 | 0.43 | 50 | 0.59 | 46 |
| 256 | 0.033 | 27 | 0.082 | 11 | 0.051 | 15 | 0.017 | 56 | 0.007 | 59 |

Table II. Calculated excitation energies $E_X$, for above target actinide products from the interactions of $^{31}P$ with $^{248}Cm$. $M$ is the total number of nucleons transferred.

| Nuclide | $M$ | $E_X$ (MeV) | Nuclide | $M$ | $E_X$ (MeV) |
|---|---|---|---|---|---|
| Bk 244 | 6 | 7.6 | Cf 246 | 6 | 6.9 |
| 245 | 5 | 11.3 | 247 | 5 | 6.3 |
| 246 | 4 | 8.6 | 248 | 4 | 8.8 |
| 247 | 3 | 10.8 | 249 | 3 | 6.7 |
| 248 | 2 | 6.4 | 250 | 2 | 7.2 |
| 249 | 1 | 6.0 | 251 | 3 | 2.5 |
| 250 | 2 | 0.0 | 252 | 4 | 0.6 |
| 251 | 3 | - 2.3 | 253 | 5 | - 8.1 |
| | | | 254 | 6 | -13.9 |
| Es 249 | 5 | 8.6 | Fm 250 | 6 | 2.4 |
| 250 | 4 | 7.1 | 251 | 5 | 4.0 |
| 251 | 3 | 9.7 | 252 | 4 | 7.2 |
| 252 | 4 | 6.1 | 253 | 5 | 5.6 |
| 253 | 5 | 5.6 | 254 | 6 | 6.2 |
| 254 | 6 | - 0.8 | 255 | 7 | 1.9 |
| 255 | 7 | - 2.5 | 256 | 8 | 0.9 |
| 256 | 8 | -14.5 | | | |

Table III. Calculated fraction of energy transferred, $F_t$, from the $^{31}P$ projectile to the $^{248}Cm$ target. $E_M$ is the maximum in the experimental excitation functions and $E_t$ is the fraction of energy transferred assuming energy transfer is proportional to mass transfer. $E_B \approx 176$ MeV in the lab frame. An * indicates that $(E_{f,n} - E_x) < 0$. See explanation in text.

| Nuclide | $E_M$ (MeV) | $F_t$ | $E_t$ | Nuclide | $E_M$ (MeV) | $F_t$ | $E_t$ |
|---|---|---|---|---|---|---|---|
| Bk 244 | 200 | * | 0.19 | Es 251 | 195 | * | 0.10 |
| 245 | 207 | * | 0.16 | 252 | 195 | * | 0.13 |
| 246 | 207 | * | 0.13 | 253 | 190 | * | 0.16 |
| 248*m* | 200 | * | 0.06 | 254*m* | 195 | 0.32 | 0.19 |
| 250 | 207 | 0.17 | 0.06 | 255 | 220 | 0.18 | 0.23 |
| Cf 246 | 207 | * | 0.19 | Fm 250 | 202 | 0.13 | 0.19 |
| 248 | 207 | * | 0.13 | 252 | 201 | * | 0.13 |
| 250 | 207 | * | 0.06 | 253 | 200 | 0.01 | 0.16 |
| 252 | 207 | 0.15 | 0.13 | 254 | 196 | * | 0.19 |
| 253 | 195 | 0.69 | 0.16 | 255 | 190 | 0.26 | 0.23 |
| | | | | 256 | 195 | 0.25 | 0.26 |

Table IV. Neutron-to-proton ratios *N/Z*, and peaks of isotopic distributions for the interactions of 253-MeV (1.08 X Coulomb barrier) $^{40}Ca$ ions, 207-MeV (1.17 X Coulomb barrier) $^{31}P$ ions, 275-MeV (1.16 X Coulomb barrier) $^{44}Ca$ ions, 245-MeV (1.16 X Coulomb barrier) $^{40}Ar$ ions, and 280-MeV (1.19 X Coulomb barrier) $^{48}Ca$ ions with $^{248}Cm$ targets. Data for $^{40,48}Ca$ taken from Ref. 2, $^{44}Ca$ taken from Ref. 3, and $^{40}Ar$ taken from Ref. 4.

| Projectile | *N/Z* | Peak of Isotopic Distributions | | | |
|---|---|---|---|---|---|
| | | Bk | Cf | Es | Fm |
| | | (Mass Number) | | | |
| $^{40}Ca$ | 1.00 | 247 | 248 | 250 | 251-252 |
| $^{31}P$ | 1.07 | 248 | 250 | 251 | 252 |
| $^{44}Ca$ | 1.20 | 248 | 250 | 251 | ≤252 |
| $^{40}Ar$ | 1.22 | 248 | 250 | 251 | ≤252 |
| $^{48}Ca$ | 1.40 | 248 | 250 | 252 | 255 |

Table V. Excitation energies, $E_x$, for Bk isotopes produced from the interactions of various heavy ions with $^{248}Cm$.

| Product Nuclide | $^{18}_{8}O$ | $^{31}_{15}P$ | $^{40}_{18}Ar$ | $^{40}_{20}Ca$ | $^{44}_{20}Ca$ | $^{48}_{20}Ca$ |
|---|---|---|---|---|---|---|
| Bk 244 | --- | 7.6 | 0.1 | 17.2 | 6.8 | -16.4 |
| 245 | -11.4 | 11.3 | 3.0 | 16.5 | 8.8 | -10.9 |
| 246 | - 9.5 | 8.6 | 1.3 | 11.9 | 5.5 | - 9.6 |
| 247 | - 4.1 | 10.8 | 2.9 | 11.1 | 5.4 | - 4.4 |
| 248 | - 4.8 | 6.4 | - 0.2 | 5.8 | 1.4 | - 5.0 |
| 249 | - 1.2 | 6.0 | 0.2 | 4.2 | 0.3 | - 3.4 |
| 250 | - 2.3 | 0.0 | - 3.2 | - 4.3 | - 4.7 | - 7.1 |
| 251 | 1.5 | - 2.3 | - 3.2 | -10.2 | - 6.0 | - 7.7 |

## FIGURE CAPTIONS

FIG. 1. Excitation functions for isotopes of Bk from the interactions of $^{31}P$ with $^{248}Cm$.

FIG. 2. Excitation functions for isotopes of Cf from the interactions of $^{31}P$ with $^{248}Cm$.

FIG. 3. Excitation functions for isotopes of Es from the interactions of $^{31}P$ with $^{248}Cm$.

FIG. 4. Excitation functions for isotopes of Fm from the interactions of $^{31}P$ with $^{248}Cm$.

FIG. 5 Isotopic distributions for Bk, Cf, Es, and Fm from the reactions of 207-Mev (1.17 X Coulomb barrier) $^{31}P$ ions with $^{248}Cm$.

FIG. 6. Isotopic distributions for Bk produced in the interactions of 207-MeV (1.17 X Coulomb barrier) $^{31}P$ ions, 245-MeV (1.16 X Coulomb barrier) $^{40}Ar$ ions, 253-MeV (1.08 X Coulomb barrier) $^{40}Ca$ ions, 275-MeV (1.16 X Coulomb barrier) $^{44}Ca$ ions, and 280-MeV (1.19 X Coulomb barrier) $^{48}Ca$ ions with $^{248}Cm$.

FIG. 7. Isotopic distributions for Cf produced in the interactions of 207-MeV (1.17 X Coulomb barrier) $^{31}P$ ions, 245-MeV (1.16 X Coulomb barrier) $^{40}Ar$ ions, 253-MeV (1.08 X Coulomb barrier) $^{40}Ca$ ions, 275-MeV (1.16 X Coulomb barrier) $^{44}Ca$ ions, and 280-MeV (1.19 X Coulomb barrier) $^{48}Ca$ ions with $^{248}Cm$.

FIG. 8. Isotopic distributions for Es produced in the interactions of 207-MeV (1.17 X Coulomb barrier) $^{31}P$ ions, 245-MeV (1.16 X Coulomb barrier) $^{40}Ar$ ions, 253-MeV (1.08 X Coulomb barrier) $^{40}Ca$ ions, 275-MeV (1.16 X Coulomb barrier) $^{44}Ca$ ions, and 280-MeV (1.19 X Coulomb barrier) $^{48}Ca$ ions with $^{248}Cm$.

FIG. 9. Isotopic distributions for Fm produced in the interactions of 207-MeV (1.17 X Coulomb barrier) $^{31}P$ ions, 245-MeV (1.16 X Coulomb barrier) $^{40}Ar$ ions, 253-MeV (1.08 X Coulomb barrier) $^{40}Ca$ ions, 275-MeV (1.16 X Coulomb barrier) $^{44}Ca$ ions, and 280-MeV (1.19 X Coulomb barrier) $^{48}Ca$ ions with $^{248}Cm$.

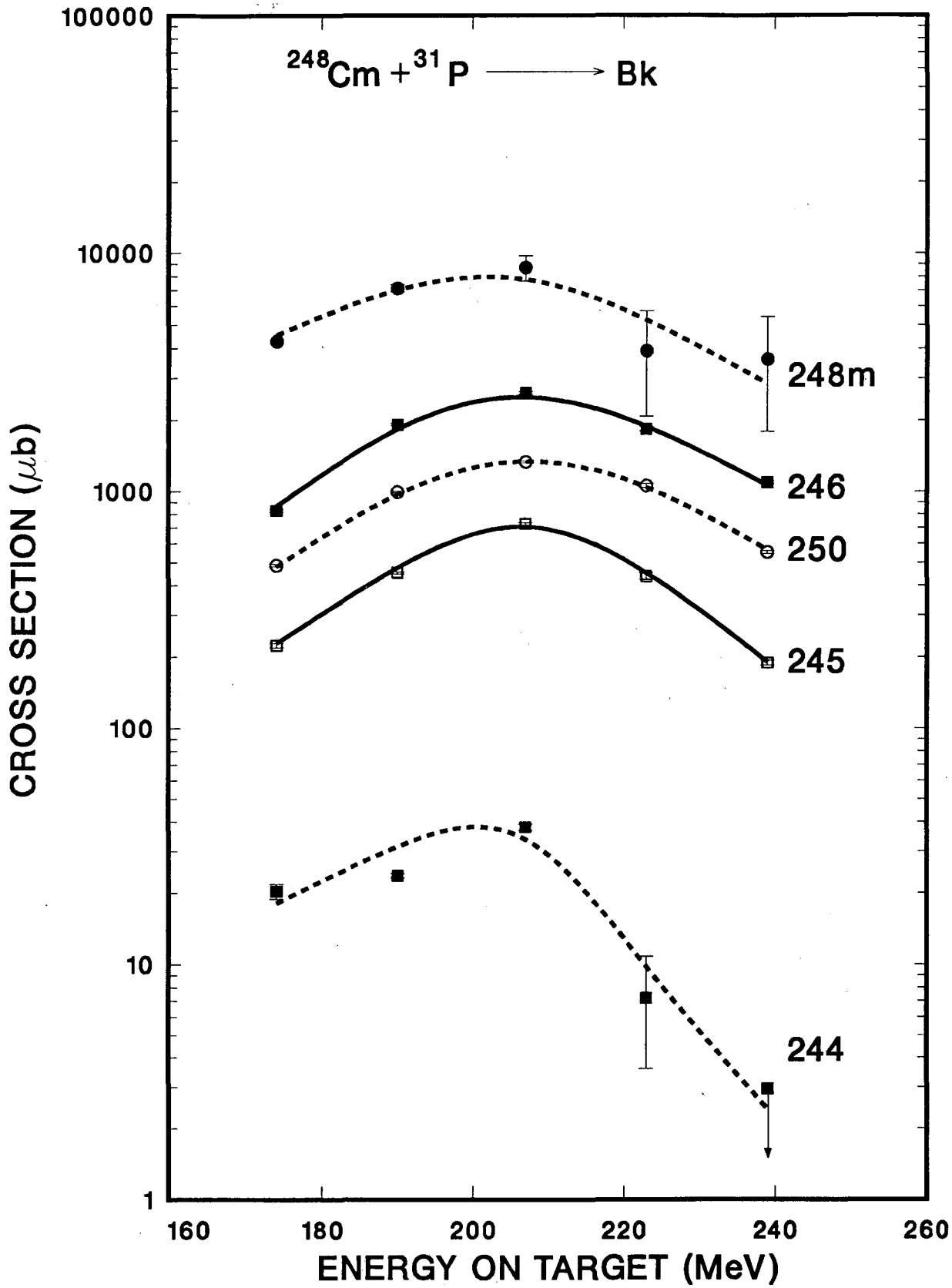
$^{248}Cm + ^{31}P \longrightarrow Bk$
248m
246
250
245
244
CROSS SECTION ($\mu b$)
100000
10000
1000
100
10
1
160
180
200
220
240
260
ENERGY ON TARGET (MeV)

Fig. 1

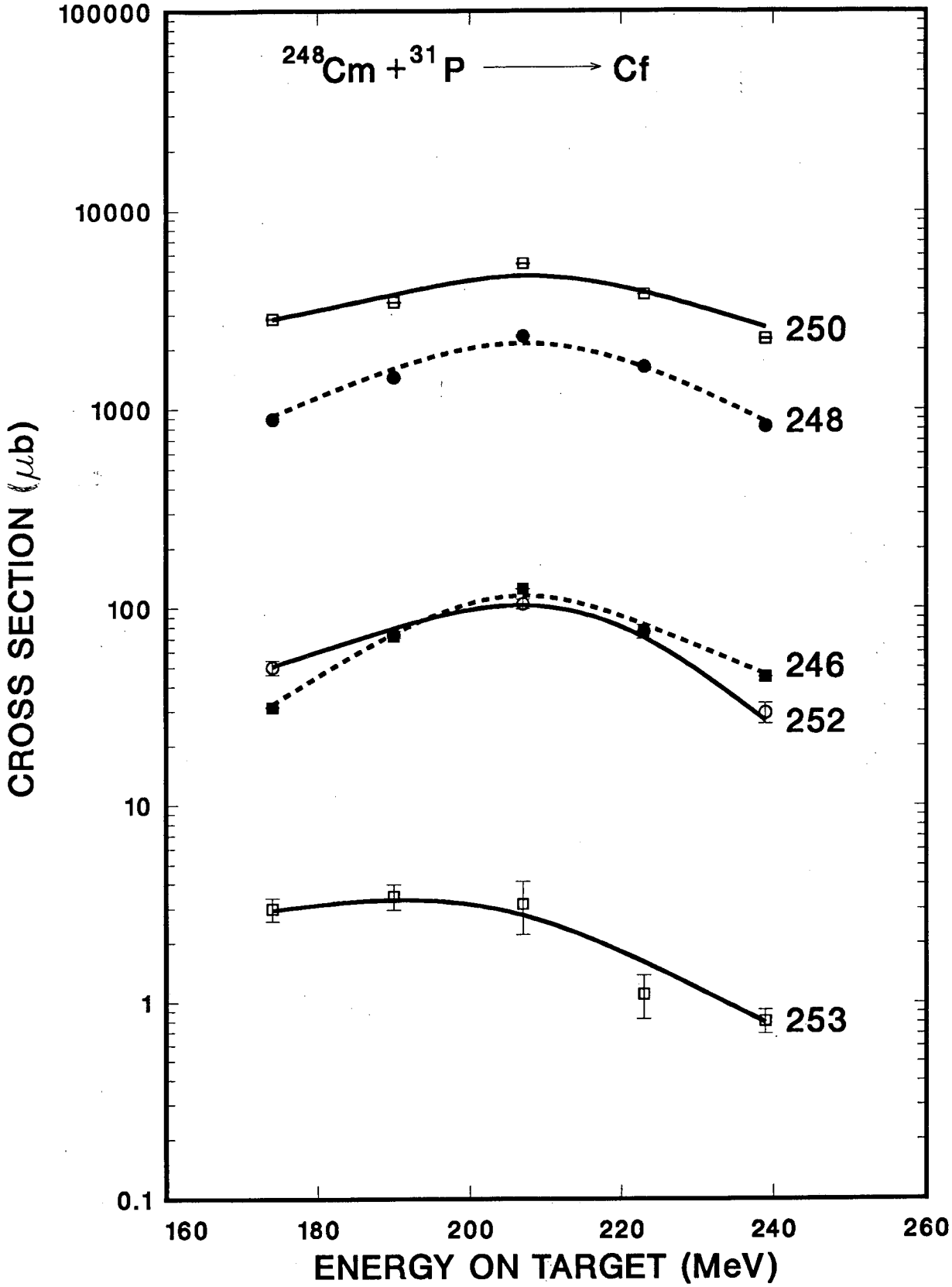
$^{248}Cm + ^{31}P \longrightarrow Cf$
100000
10000
1000
100
10
1
0.1
CROSS SECTION ($\mu$b)
160
180
200
220
240
260
ENERGY ON TARGET (MeV)
250
248
246
252
253

Fig. 2

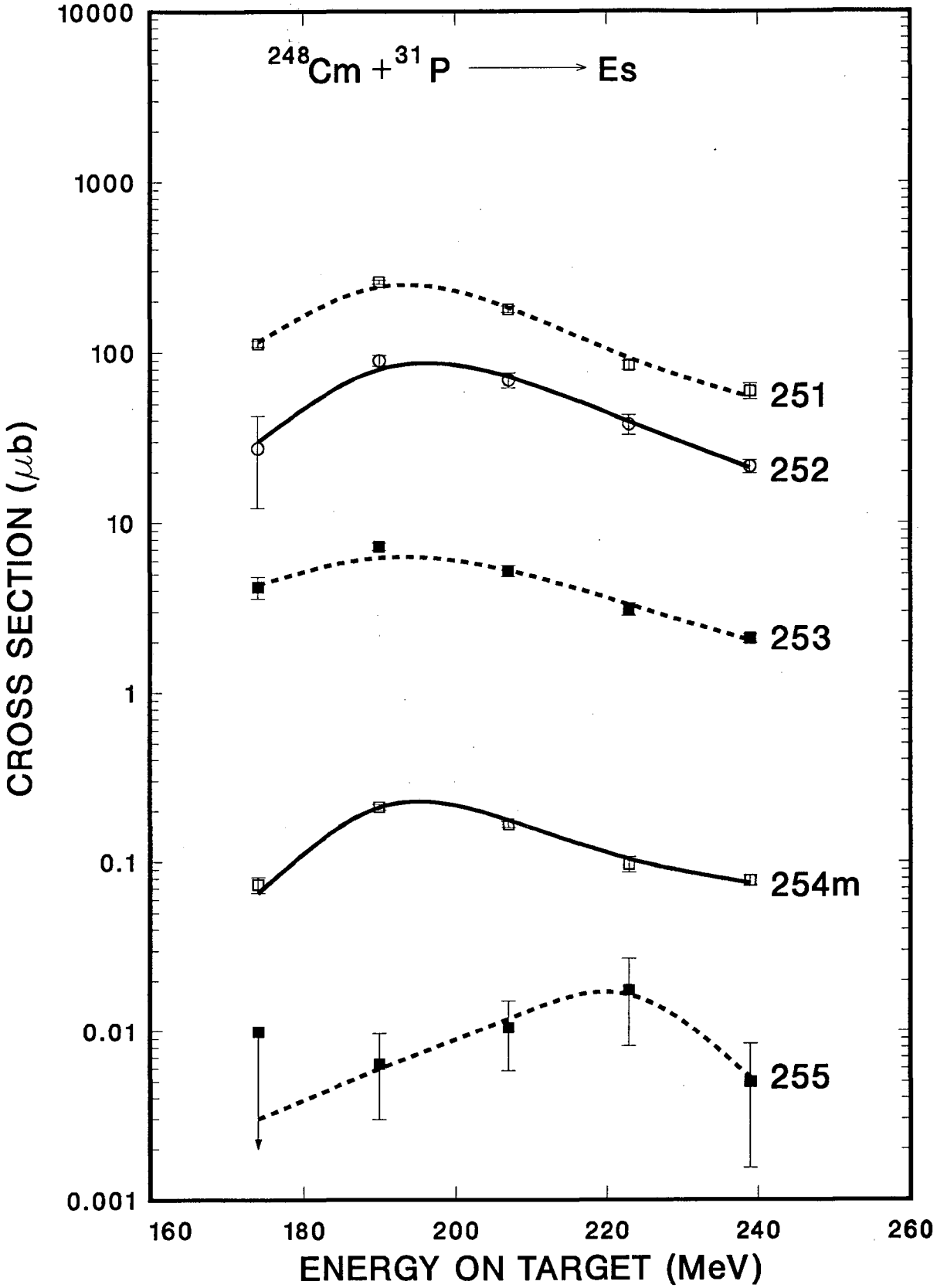
$^{248}Cm + ^{31}P \longrightarrow Es$
10000
1000
100
10
1
0.1
0.01
0.001
CROSS SECTION ($\mu$b)
251
252
253
254m
255
160
180
200
220
240
260
ENERGY ON TARGET (MeV)

Fig. 3

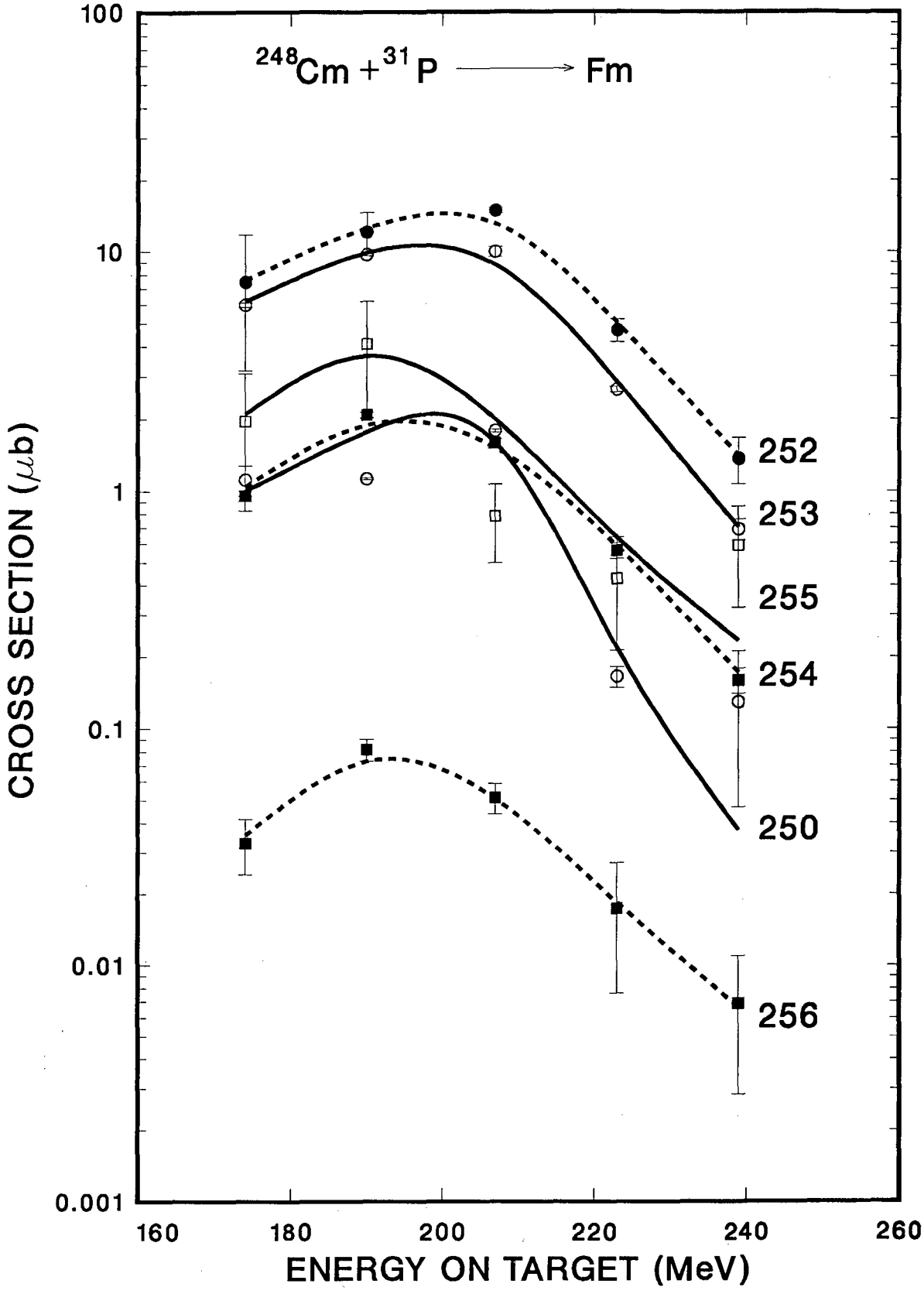
$^{248}Cm + ^{31}P \longrightarrow Fm$
CROSS SECTION ($\mu$b)
100
10
1
0.1
0.01
0.001
160
180
200
220
240
260
ENERGY ON TARGET (MeV)
252
253
255
254
250
256

Fig. 4

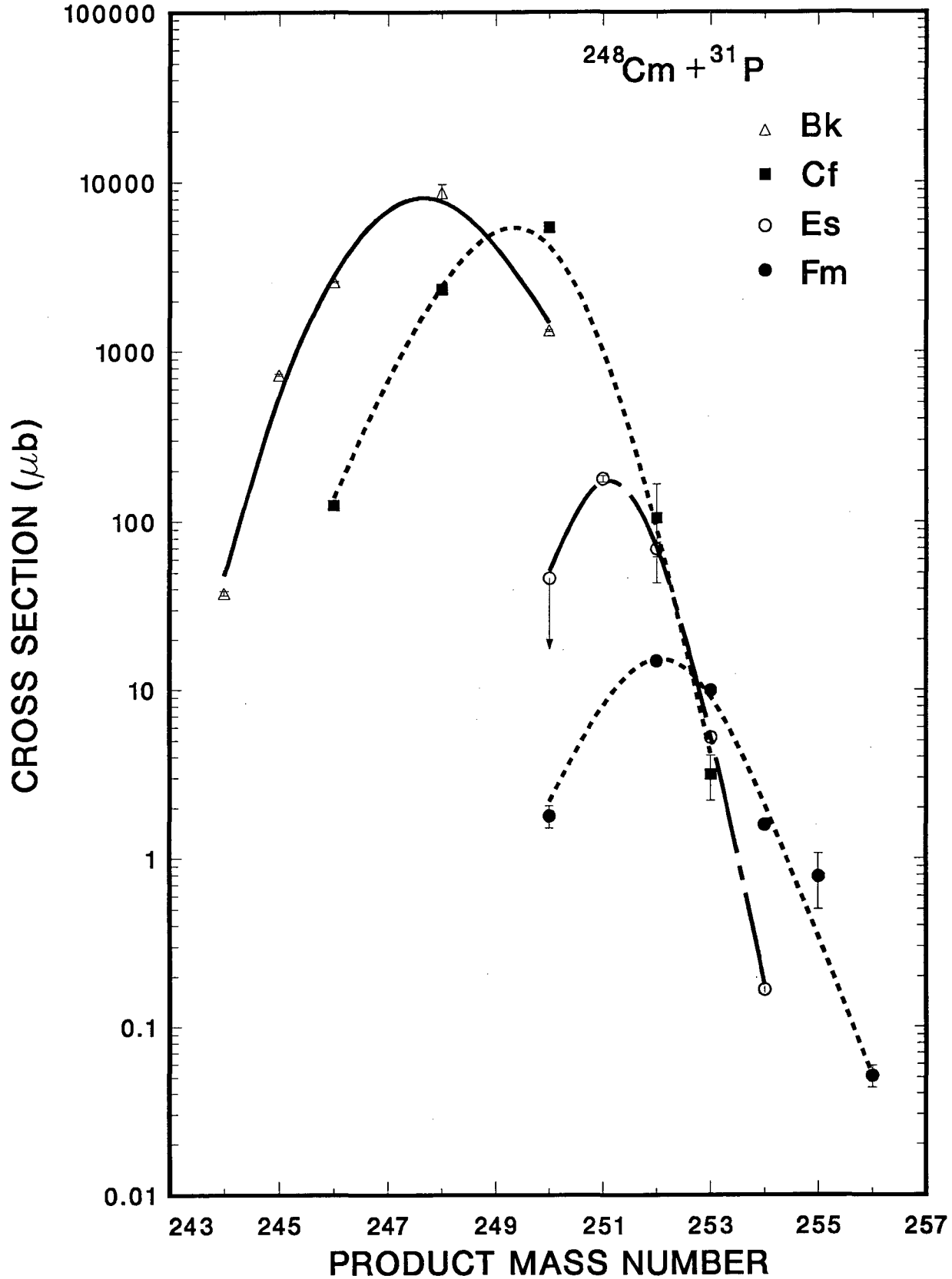
$^{248}Cm + ^{31}P$
Bk
Cf
Es
Fm
CROSS SECTION ($\mu$b)
100000
10000
1000
100
10
1
0.1
0.01
243
245
247
249
251
253
255
257
PRODUCT MASS NUMBER

Fig. 5

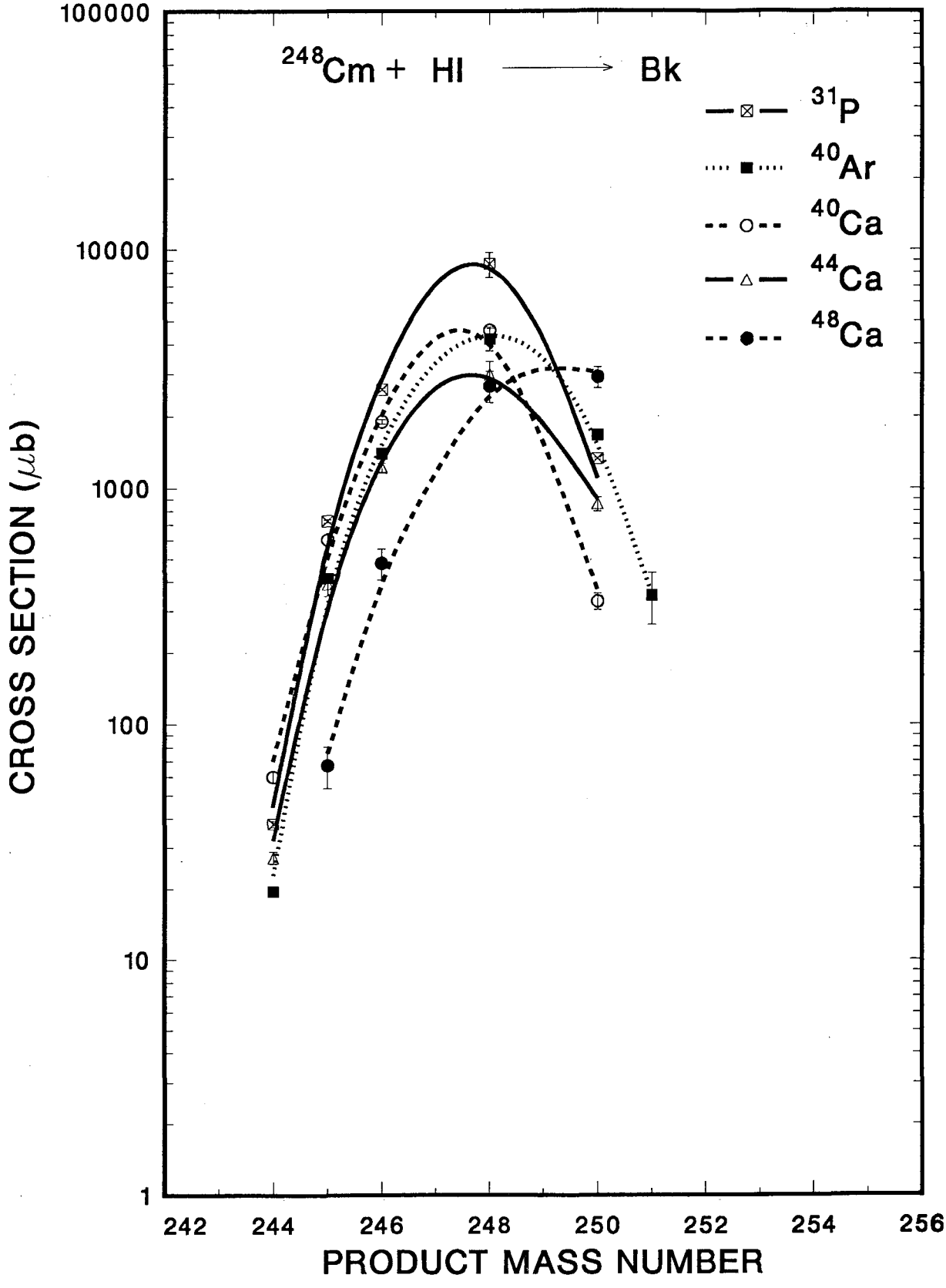
$^{248}$Cm + HI ⟶ Bk
$^{31}$P
$^{40}$Ar
$^{40}$Ca
$^{44}$Ca
$^{48}$Ca
CROSS SECTION (μb)
100000
10000
1000
100
10
1
242
244
246
248
250
252
254
256
PRODUCT MASS NUMBER

Fig. 6

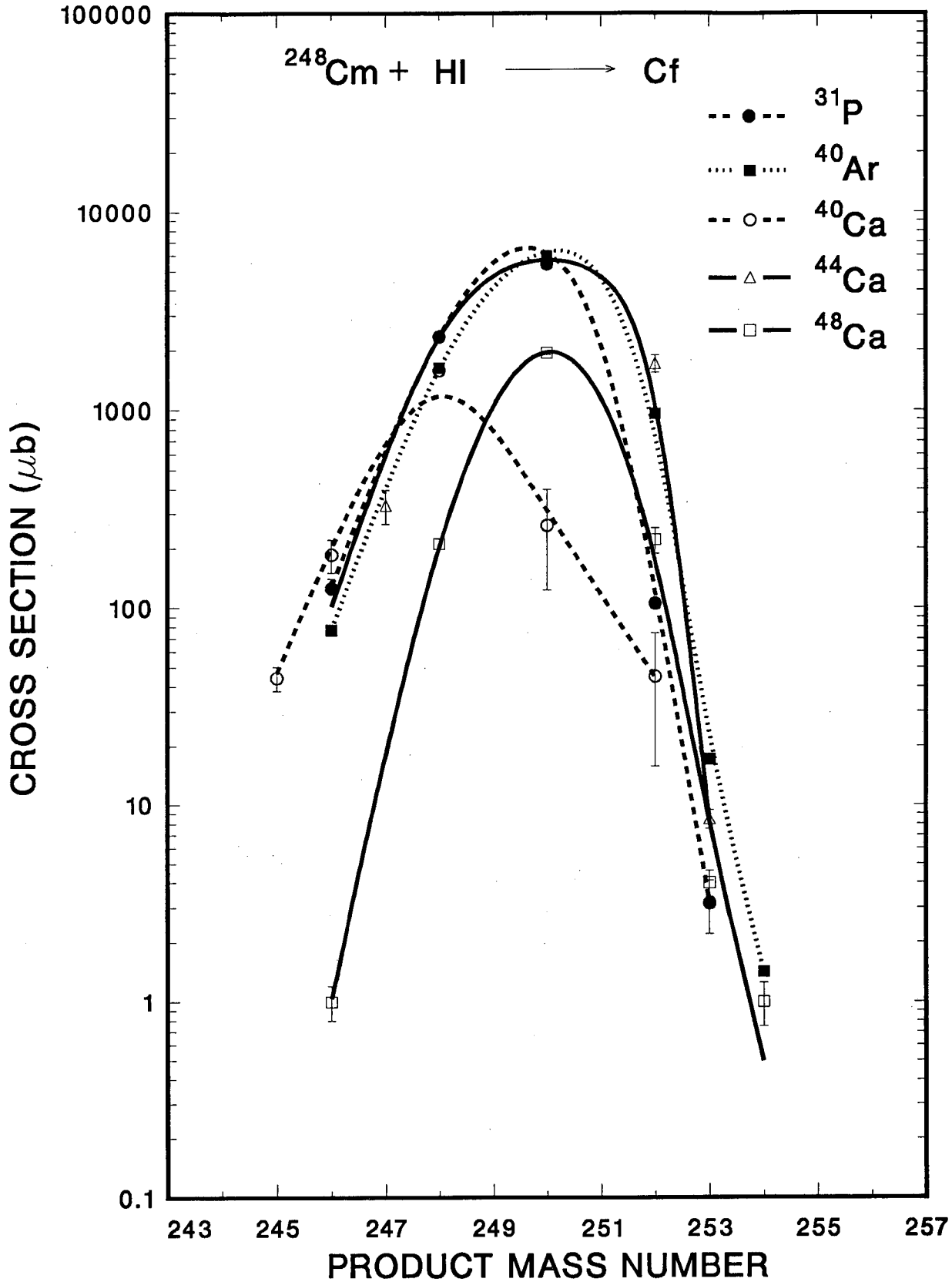
$^{248}$Cm + HI ⟶ Cf
$^{31}$P
$^{40}$Ar
$^{40}$Ca
$^{44}$Ca
$^{48}$Ca
CROSS SECTION ($\mu$b)
100000
10000
1000
100
10
1
0.1
243
245
247
249
251
253
255
257
PRODUCT MASS NUMBER

Fig. 7

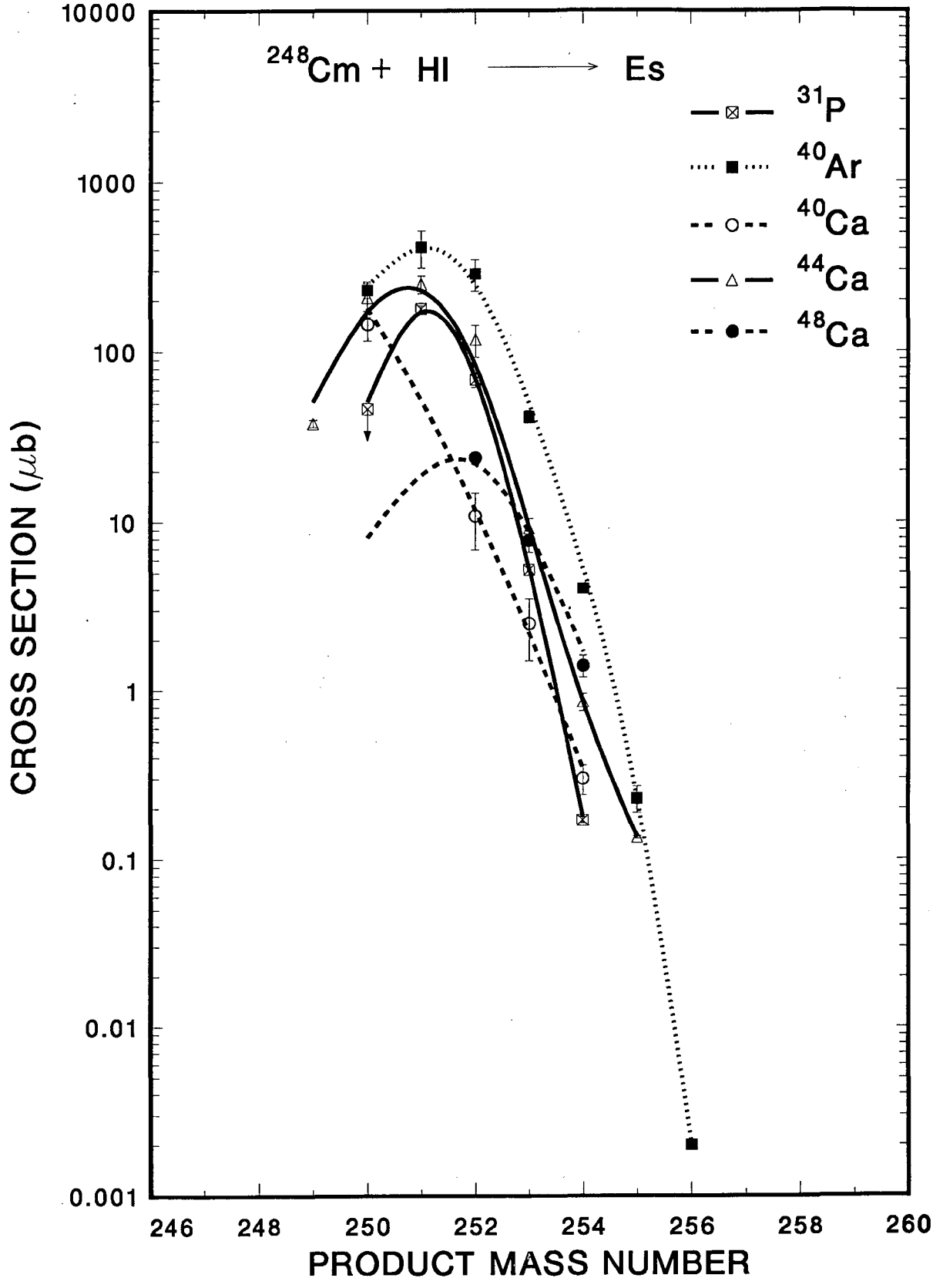
$^{248}$Cm + HI ⟶ Es
$^{31}$P
$^{40}$Ar
$^{40}$Ca
$^{44}$Ca
$^{48}$Ca
CROSS SECTION ($\mu$b)
10000
1000
100
10
1
0.1
0.01
0.001
246
248
250
252
254
256
258
260
PRODUCT MASS NUMBER

Fig. 8

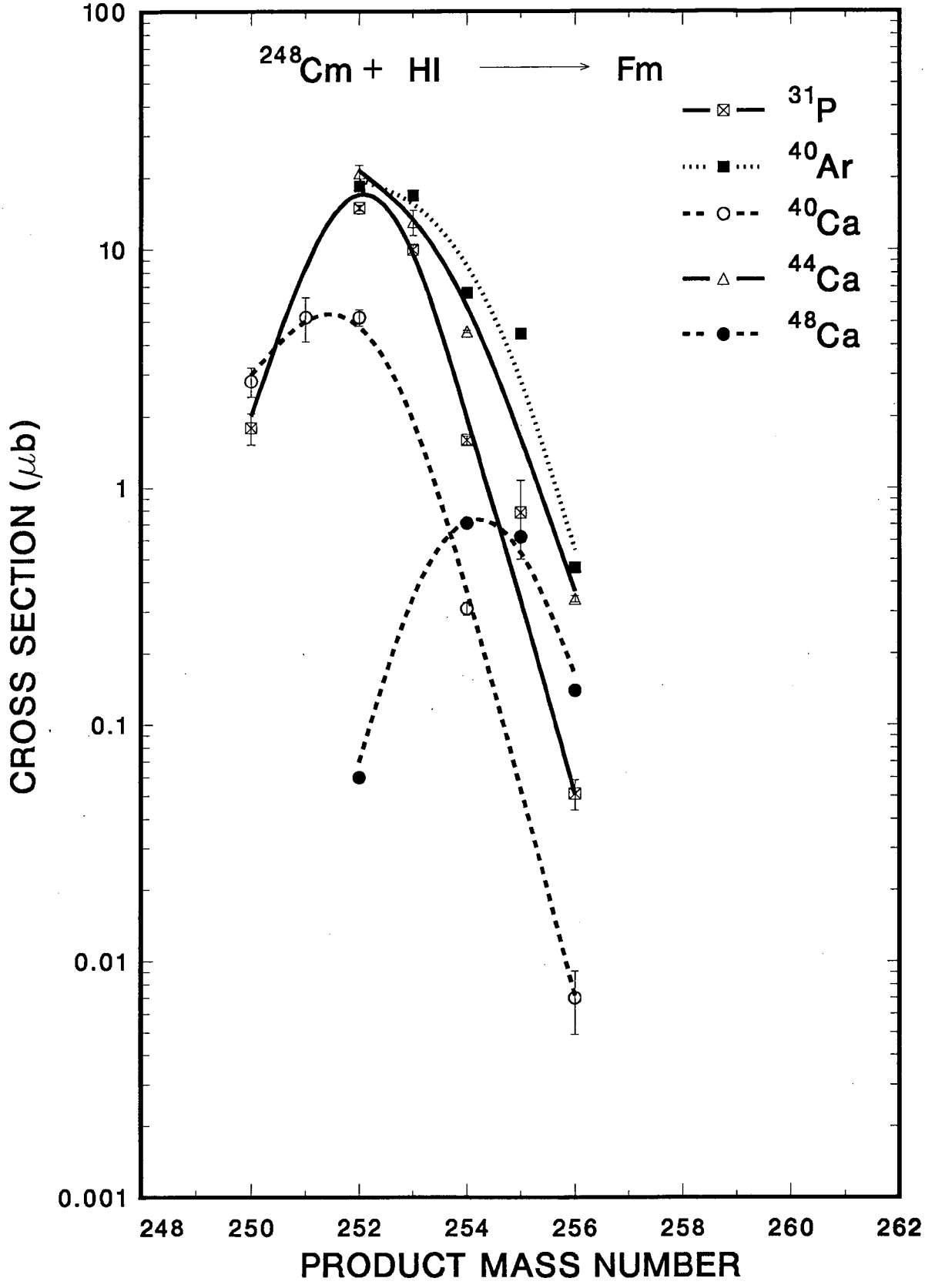
$^{248}$Cm + HI ⟶ Fm
$^{31}$P
$^{40}$Ar
$^{40}$Ca
$^{44}$Ca
$^{48}$Ca
CROSS SECTION ($\mu$b)
100
10
1
0.1
0.01
0.001
248
250
252
254
256
258
260
262
PRODUCT MASS NUMBER

Fig. 9

LAWRENCE BERKELEY LABORATORY
UNIVERSITY OF CALIFORNIA
INFORMATION RESOURCES DEPARTMENT
1 CYCLOTRON ROAD
BERKELEY, CALIFORNIA 94720